Electrochromic Conducting Polymers via Electrochemical Polymerization of Bis(2-(3,4-ethylenedioxy)thienyl) Monomers

Gregory A. Sotzing and John R. Reynolds*

Department of Chemistry, Center for Macromolecular Science and Engineering, University of Florida, Gainesville, Florida 32611

Peter J. Steel

Department of Chemistry, University of Canterbury, Christchurch, New Zealand

Received October 11, 1995. Revised Manuscript Received January 30, 1996[⊗]

A series of bis(2-(3,4-ethylenedioxy)thiophene)-based monomers have been synthesized and fully characterized; specifically (*E*)-1,2-bis(2-(3,4-ethylenedioxy)thienyl)vinylene (BEDOT-V), 1,4-bis(2-(3,4-ethylenedioxy)thienyl)benzene (BEDOT-B), 4,4′-bis(2-(3,4-ethylenedioxy)-thienyl)biphenyl (BEDOT-BP), 2,5-bis(2-(3,4-ethylenedioxy)thienyl)furan (BEDOT-F), 2,5-bis(2-(3,4-ethylenedioxy)thienyl)-thiophene (BEDOT-T), and 2,2′:5′,2″-ter(3,4-ethylenedioxy)thiophene, TER-EDOT. The X-ray crystal structures of BEDOT-V and BEDOT-B have been determined. These monomers oxidize and polymerize at low potentials relative to other reported electropolymerizable heterocycles. The electroactive polymers formed exhibit low redox switching potentials and are quite stable in the conducting state. TER-EDOT was found to have the lowest peak oxidation potential of +0.2 V vs Ag/Ag^+, making it the most easily oxidized polymerizable thiophene monomer reported. The electronic bandgaps of these EDOT based polymers range from 1.4 to 2.3 eV (measured as the onset of the $\pi-\pi^*$ transition) offering a diverse range of colors which may prove useful in electrochromic devices. For example, poly(BEDOT-V) is deep purple and opaque in the reduced state and transmissive sky blue in the oxidized state, poly(BEDOT-T) is deep blue opaque in the reduced state and transmissive blue in the oxidized state, while poly(BEDOT-BP) is transmissive orange in the reduced state and opaque purple in the oxidized state. A thin film of poly(BEDOT-V) was found to switch rapidly between redox states (under 2 s) with an initial optical contrast of 43%. This polymer was found to retain 47% of its optical contrast and 48% of its original charge density after 600 double potential steps.

Introduction

Thiophene-based polymers and oligomers have received significant attention for their unique electrical properties and ability to exhibit environmental stabilities necessary for a number of practical applications. For example, these materials have been used as charge dissipation coatings in electron-beam lithography,[1] and as an active semiconducting material in organic thin-film transistors.[2] Recently, Shi and co-workers reported the preparation of tough and mechanically durable polythiophene films from the electrochemical polymerization of thiophene from a boron trifluoride−diethyl ether solution, such that the films had a tensile strength greater than that of aluminum.[3]

A number of studies have focused on thiophene based polymers as potential materials for electrochromic devices.[4−9] An electrochromic material possesses the ability to reversibly change color by altering its redox state. Poly(3-methylthiophene) is known to be blue in the oxidized state and red in the reduced state. Panero et al. have investigated electrochromic devices using poly(3-methylthiophene) coated ITO glass electrodes and obtained an optical contrast between the reduced and oxidized states of about 30%.[6]

3,4-Ethylenedioxythiophene (EDOT) is a commercially available, oxidatively polymerizable monomer which polymerizes at relatively low applied potentials (+1.0 V vs Ag/Ag^+).[10] Syntheses of EDOT were originally reported by Fager[11] and Gogte et al.[12] Heywang and Jonas first polymerized EDOT to poly(3,4-ethylenedioxythiophene) [poly(EDOT)] and found the polymer to be useful for antistatic coatings.[10,13] Heinze and co-workers subsequently studied the spectroscopic and electrochemical properties of poly(EDOT) and found the polymer to have a low half wave potential ($E_{1/2,p}$) of

[⊗] Abstract published in *Advance ACS Abstracts,* March 1, 1996.

(1) Huang, W.-S. *Polymer* **1994**, *35*, 4057.
(2) Dodabalapur, A.; Torsi, L.; Katz, H. E. *Science* **1995**, *268*, 270.
(3) Shi, G.; Jin, S.; Xue, G.; Li, C. *Science* **1995**, *267*, 994.
(4) Druy, M. A.; Seymour, R. J. *J. Phys.* **1983**, *C3*, 595.
(5) Haynes, D. M.; Hepburn, A. R.; Goldie, D. M.; Marshall, J. M.; Pelter, A. *Synth. Met.* **1993**, *55−57*, 839−844.
(6) Panero, S.; Passerini, S.; Scrosati, B. *Mol. Cryst. Liq. Cryst.* **1993**, *229*, 97.
(7) Gustafsson, J. C.; Inganas, O.; Andersson, A. M. *Synth. Met.* **1994**, *62*, 17.
(8) Hyodo, K. *Electrochim. Acta* **1994**, *39*, 265.
(9) Nawa, K.; Imae, I.; Noma, N.; Shirota, Y. *Macromolecules* **1995**, *28*, 723.
(10) Jonas, F.; Heywang, G.; Gladbach, B.; Schmidtberg, W.; Heinze, J.; Dietrich, M. U.S. Patent No. 5,035,926.
(11) Fager, E. W. *J. Am. Chem. Soc.* **1945**, *67*, 2217.
(12) Gogte, V. N.; Shah, L. G.; Tilak, B. D.; Gudekar, K. N.; Schasrabudhe, M. B. *Tetrahedron* **1967**, *23*, 2437.
(13) (a) Heywang, G.; Jonas, F. *Adv. Mater.* **1992**, *4*, 116. (b) Heywang, G.; Jonas, F. *Electrochim. Acta* **1994**, *39*, 1345.

0897-4756/96/2808-0882$12.00/0

−0.25 V vs Ag/AgCl.[14] Optoelectrochemical analysis indicated that the polymer has an optical bandgap of ca. 1.6 eV (760−780 nm). Inganas and co-workers showed the usefulness of poly(EDOT) as a potential material for electrochromic devices due to its ability to cycle between an opaque blue-black in the reduced (undoped) state and a transmissive sky blue in the oxidized (doped) state.[15] Conductivities reported for poly(EDOT) prepared electrochemically range from 10 to 100 S cm^{-1}, and these conductivites have been found to be stable for up to 1000 h at 120 °C in a laboratory atmosphere.[13a]

Previously, it has been shown that bis-heterocycle-substituted arylene monomers easily electrochemically polymerize to form stable electroactive polymers.[16,17] Assembly of a three-ring monomer increases the conjugation length and significantly lowers the oxidation potential at which it polymerizes. By lowering the oxidation potential, side reactions such as β coupling and overoxidation of the polymer can be avoided. These polymers can be more ordered and have been shown to exhibit bandgaps lower than their parent polyheterocycle.[16b] For the above reasons, we chose EDOT as the external heterocyclic rings for easily electropolymerized monomers designed to yield electroactive and electrochromic polymers which switch at low potentials.

We have communicated on the synthesis and electrochemical polymerization of (*E*)-1,2-bis(2-(3,4-ethylenedioxy)thienyl)vinylene (BEDOT-V), 1,4-bis(2-(3,4-ethylenedioxy)thienyl)benzene (BEDOT-B), and 4,4′-bis(2-(3,4-ethylenedioxy)-thienyl)biphenyl (BEDOT-BP).[18] Poly(BEDOT-V) exhibits an optical bandgap of 1.4 eV and switches between purple opaque and sky blue transmissive states, potentially useful for electrochromic devices. Elsenbaumer also reported the synthesis and electrochemical polymerization of BEDOT-V and found the polymer to have a bandgap of 1.4 eV.[19]

This paper details the synthesis, electropolymerization, and electrochemical properties (cyclic voltammetry, optoelectrochemistry, and electrochromic switching) of BEDOT-V, BEDOT-B, and BEDOT-BP along with three additional monomers, 2,5-bis(2-(3,4-ethylenedioxy)thienyl)furan (BEDOT-F), 2,5-bis(2-(3,4-ethylenedioxy)thienyl)-thiophene (BEDOT-T), and 2,2′:5′,2″-ter(3,4-ethylenedioxy)thiophene (TER-EDOT). We demonstrate the utility of these polymers as electrochromic materials with a range of accessible colors which is attributed to the structural control of electronic properties.

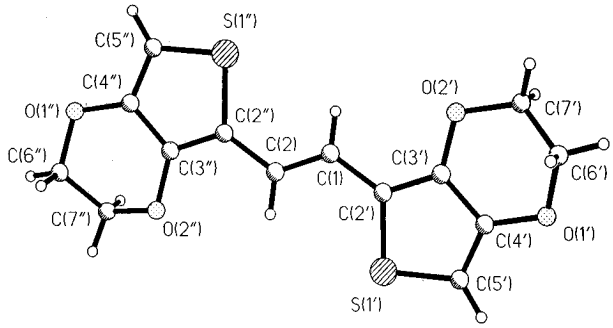

Figure 1. Perspective view and atom labeling of the crystal structure of BEDOT-V.

Scheme 1

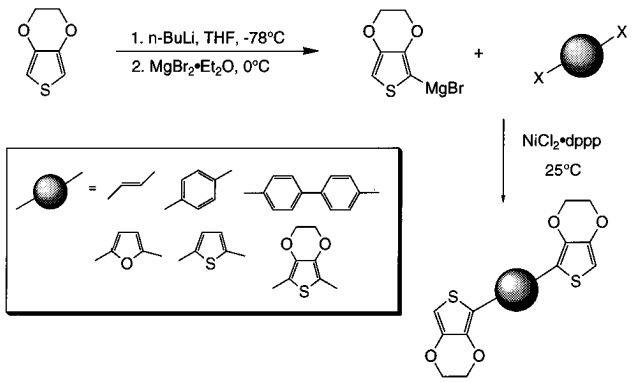

Results and Discussion

Monomer Synthesis. BEDOT−arylene monomers were prepared via a $NiCl_2$•dppp-catalyzed Grignard coupling with the corresponding dihalo compound as illustrated in Scheme 1. It should be noted that aryl bromides reacted much faster than *trans*-dichloroethylene making it necessary to increase the reaction time for the preparation of BEDOT-V. High yields (ca. 60−80%) were obtained for both the aryl dibromide−Grignard and the dichloroethylene−Grignard couplings. All monomers were fully characterized using ^1H and ^{13}C NMR, FAB-HRMS, UV−Vis spectrophotometry, elemental analysis, and melting points.

Structural Analysis. The structures of BEDOT-V and BEDOT-B were determined by single-crystal X-ray crystallography in order to examine torsional angles in the conjugated systems. Figures 1 and Figure 2 show perspective views, approximately perpendicular to the molecular mean planes, and atom labeling of the two structures. Table 1 lists the crystal data, collection, and refinement parameters, and Tables 2 and 3 list the final atomic coordinates. Bond lengths and angles are given in Tables 4 and 5.

BEDOT-V crystallizes in the monoclinic space group $P2_{1/n}$ with a full molecule in the asymmetric unit. There is minor disorder of two of the methylene carbons (C6′ and C7″) of the six-membered rings that is not shown in Figure 1. The molecule is essentially planar with the mean planes of the two thiophene rings being inclined to the plane of the central double bond at angles of 4.2-

(14) Dietrich, M.; Heinze, J.; Heywang, G.; Jonas, F. *J. Electroanal. Chem.* **1994**, *369*, 87.
(15) Pei, Q.; Zuccarello, G.; Ahlskog, M.; Inganas, O. *Polymer* **1994**, *35*, 1347.
(16) (a) Child, A. D.; Sankaran, B.; Larmat, F.; Reynolds, J. R. *Macromolecules*, in press. (b) Reynolds, J. R.; Katritzky, A. R.; Soloducho, J.; Belyakov, S.; Sotzing, G.; Pyo, M. *Macromolecules* **1994**, *27*, 7225. (c) Reynolds, J. R.; Child, A. D.; Ruiz, J. P.; Hong, S. Y.; Marynick, D. S. *Macromolecules* **1993**, *26*, 2095. (d) Ruiz, J. P.; Dharia, J. R.; Reynolds, J. R.; Buckley, L. J. *Macromolecules* **1992**, *25*, 849. (e) Reynolds, J. R.; Ruiz, J. P.; Child, A. D.; Nayak, K.; Marynick, D. S. *Macromolecules* **1991**, *24*, 678.
(17) (a) Danieli, R.; Ostoja, R.; Tiecco, M.; Zamboni, R.; Taliani, C. *J. Chem. Soc., Chem. Commun.* **1986**, 1473. (b) Ferraris, J. P.; Skiles, G. D. *Polymer* **1987**, *28*, 179. (c) Tanaka, S.; Kaeriyama, K.; Hiraide, T. *Makromol. Chem., Rapid Commun.* **1988**, *9*, 743. (d) Kaeriyama, K.; Tanaka, S. *Makromol. Chem.* **1988**, *189*, 1755. (e) Ferraris, J. P.; Andrus, R. G.; Hrncir, D. C. *J. Chem. Soc., Chem. Commun.* **1989**, 1318. (f) Pelter, A.; Maud, J. M.; Jenkins, I.; Sadeka, C.; Coles, G. *Tetrahedron Lett.* **1989**, *30*, 3461. (g) Roncali, J.; Gorgues, A.; Jubault, M. *Chem. Mater.* **1993**, *5*, 1456. (h) Haynes, P. M.; Hepburn, A. R.; Goldie, D. M.; Marshall, J. M.; Pelter, A. *Synth. Met.* **1993**, *55−57*, 839. (i) Lorcy, D.; Cava, M. P. *Adv. Mater.* **1992**, *4*, 562. (j) Kitamura, C.; Tanaka, S.; Yamashita, Y. *J. Chem. Soc., Chem. Commun.* **1994**, 1585.
(18) (a) Sotzing, G. A.; Reynolds, J. R. *J. Chem. Soc., Chem. Commun.* **1995**, 703. (b) Sotzing, G. A.; Reynolds, J. R.; Katritzky, A. R.; Soloducho, J.; Musgrave, R. *Proc. Am. Chem. Soc., Div. Polym. Mater.: Sci. Eng.* **1995**, *72*, 318.
(19) Fu, Y.; Elsenbaumer, R. L. *Proc. Am. Chem. Soc., Div. Polym. Mater.: Sci. Eng.* **1995**, *72*, 315.

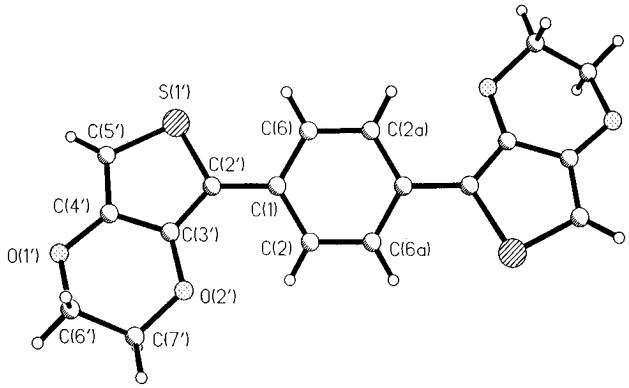

Figure 2. Perspective view and atom labeling of the crystal structure of BEDOT-B.

Table 1. Crystal Data and Collection and Refinement Parameters

	BEDOT-V	BEDOT-B
molecular formula	$C_{14}H_{12}O_4S_2$	$C_{18}H_{14}O_4S_2$
molecular mass	308.36	358.41
crystal system	monoclinic	orthorhombic
a, Å	9.415(4)	10.383(2)
b, Å	10.389(5)	9.263(1)
c, Å	14.236(6)	15.538(2)
β, deg	91.24(3)	90
V, Å^3	1392(1)	1494.4(4)
space group	$P2_1/n$	Pbca
Z	4	4
D_x, g cm^{-3}	1.471	1.593
crystal form	orange block	tan plate
crystal dimensions, mm	0.75 × 0.32 × 0.16	0.68 × 0.47 × 0.04
μ, cm^{-1}	3.91	3.77
temp, K	293	130
2θ range, deg	4−50	4−50
data collected	$+h, +k, \pm l$	$+h, +k, +l$
reflns measured	2446	1172
reflns with $I > 2\sigma(I)$	1487	819
weighting factor *a*	0.0575	0.0409
parameters refined	201	109
R_w (all data)	0.100	0.072
R_1 [$I > 2\sigma(I)$]	0.039	0.031
diff Fourier min/max (e Å^3)	+0.20/−0.18	+0.25/−0.19

(2) and 1.4(2)° and mutually inclined at an angle of 5.1-(2)°. The maximum deviations (of approximately 0.5 Å) from the molecular mean plane are exhibited by the disordered methylene carbons.

BEDOT-B crystallizes in the orthorhombic space group *Pbca* with half a molecule in the asymmetric unit, the other half being generated by a crystallographic center of inversion. In this case, the molecule deviates significantly from planarity, with the central benzene ring being inclined to the plane of the attached thiophene rings at an angle of 27.5(2)°. The six-membered dioxane ring exists in a half-chair conformation with no disorder of the methylene carbons. In neither structure are there any intermolecular contacts between nonhydrogen atoms of less than 3.2 Å.

The structure of the monomer in the solid state can be related to the structure of the repeat unit of the neutral polymer. From the above results, poly(BEDOT-V) will have an essentially planar repeat unit with an increased degree of conjugation compared to poly-(BEDOT-B). It is known that as the ability of the neutral polymer to attain a planar conformation increases, less energy is needed to stabilize the bipolaron state upon oxidation of the polymer. Also, the more planar the polymer in the solid state, the higher the possibility of interchain transport occurring. This suggests that poly(BEDOT-V) should have a lower $\pi-\pi^*$ transition than poly(BEDOT-B). For the case of BEDOT-B, the torsional angle between rings is substantially larger. This causes a reduction in the degree of conjugation, leading to an increased energy for the $\pi-\pi^*$ transition. Crystals of BEDOT-T and TER-EDOT were not of sufficient size and quality for single-crystal structure determination.

Table 2. Atomic Coordinates [×10^4] and Equivalent Isotropic Displacement Parameters [Å^2 × 10^3] for BEDOT-V

	x	*y*	*z*	*U*(eq)
C(1)	3381(3)	10880(3)	5782(2)	46(1)
C(2)	3816(3)	11320(2)	6624(2)	44(1)
S(1′)	5197(1)	12417(1)	4727(1)	53(1)
C(2′)	3854(3)	11291(2)	4878(2)	42(1)
C(3′)	3359(3)	10887(2)	4015(2)	43(1)
C(4′)	4014(3)	11494(3)	3249(2)	48(1)
C(5′)	5027(3)	12338(3)	3527(2)	56(1)
O(1′)	3654(2)	11234(2)	2330(1)	65(1)
O(2′)	2303(2)	9996(2)	3907(1)	55(1)
C(6′A)[a]	2294(10)	10614(11)	2270(3)	77(3)
C(6′B)[b]	2934(33)	9980(25)	2256(12)	56(6)
C(7′)	2073(5)	9644(4)	2956(2)	96(1)
S(1′)	2142(1)	9650(1)	7662(1)	60(1)
C(2″)	3357(3)	10883(2)	7525(2)	43(1)
C(3″)	3797(3)	11317(2)	8388(2)	42(1)
C(4″)	3162(3)	10683(3)	9152(2)	45(1)
C(5″)	2233(3)	9760(3)	8865(2)	60(1)
O(1″)	3457(2)	10965(2)	10069(1)	58(1)
O(2″)	4771(2)	12282(2)	8514(1)	53(1)
C(6″)	4318(4)	12081(4)	10168(2)	81(1)
C(7″A)[c]	5347(7)	12244(7)	9459(3)	63(2)
C(7″B)[d]	4568(21)	12965(15)	9421(7)	53(5)

[a] Disordered; site occupancy 80%. [b] Disordered; site occupancy 20%. [c] Disordered; site occupancy 75%. [d] Disordered; site occupancy 25%.

Table 3. Atomic Coordinates [×10^4] and Equivalent Isotropic Displacement Parameters [Å^2 × 10^3] for BEDOT-B

	x	y	z	U(eq)
C(1)	5249(2)	6392(2)	4669(2)	18(1)
C(2)	4604(2)	5358(2)	4174(2)	21(1)
C(6)	5635(2)	6011(2)	5501(2)	21(1)
S(1′)	6785(1)	8860(1)	4699(1)	24(1)
C(2′)	5495(2)	7842(2)	4324(2)	19(1)
C(3′)	4821(2)	8617(2)	3730(2)	19(1)
C(4′)	5328(2)	10030(2)	3591(2)	21(1)
C(5′)	6383(2)	10314(2)	4069(2)	24(1)
O(1′)	4796(2)	10980(2)	3014(1)	26(1)
O(2′)	3701(2)	8153(2)	3354(1)	23(1)
C(6′)	3508(2)	10579(3)	2773(2)	29(1)
C(7′)	3399(2)	8992(2)	2595(2)	26(1)

Monomer Oxidation. The first anodic scan for each of the monomers was carried out under identical electrochemical conditions in order to determine the effect of monomer structure on oxidation properties. Table 6 contains the onset potentials for the oxidation of each monomer ($E_{onset,m}$) and their peak oxidation potentials ($E_{p,m}$). Using TER-EDOT as an example, monomer oxidation occurs with an $E_{p,m}$ at 0.20 V and an $E_{onset,m}$ of 0.15 V vs Ag/Ag$^+$ (all further potentials are reported versus this reference electrode). Importantly, this is 0.85 V lower than the E_{onset} of EDOT. In fact, this monomer oxidizes at a potential lower than that of the thiophene pentamer.[20] We believe TER-EDOT to be the most easily oxidized and polymerized thiophene-based monomer reported to date.

(20) Parakka, J. P.; Cava, M. P. *Synth. Met.* **1995**, *68*, 275.

Table 4. Bond Lengths (Å) and Angles (deg) for BEDOT-V

C(1)−C(2)	1.340(3)	C(1)−C(2′)	1.436(2)	C(2)−C(2″)	1.436(3)
S(1′)−C(5′)	1.715(3)	S(1′)−C(2′)	1.739(3)	C(2′)−C(3″)	1.370(3)
C(3′)−O(2′)	1.364(3)	C(3′)−C(4′)	1.412(4)	C(4′)−C(5′)	1.348(4)
C(4′)−O(1′)	1.371(3)	O(1′)−C(6′A)[a]	1.435(6)	C(1′)−C(6′B)[b]	1.47(2)
O(2′)−C(7′)	1.415(3)	C(6′A)[a]−C(7′)	1.421(8)	C(6′B)[b]−C(7′)	1.34(2)
S(1″)−C(5″)	1.717(3)	S(1″)−C(2″)	1.731(3)	C(2″)−C(3″)	1.365(3)
C(3″)−O(2″)	1.368(3)	C(3″)−C(4″)	1.414(3)	C(4″)−C(5″)	1.355(4)
C(4″)−O(1″)	1.361(3)	O(1″)−C(6″)	1.420(4)	O(2″)−C(7″A)[c]	1.439(4)
O(2″)−C(7″B)[d]	1.489(13)	C(6″)−C(7″A)[c]	1.425(5)	C(6″)−C(7″B)[d]	1.428(12)

C(2)−C(1)−C(2′)	127.3(3)	C(1)−C(2)−C(2″)	126.8(3)
C(5′)−S(1′)−C(2′)	92.18(13)	C(3′)−C(2′)−C(1)	127.3(2)
C(3′)−C(2′)−S(1′)	109.3(2)	C(1)−C(2′)−S(1′)	123.4(2)
O(2′)−C(3′)−C(2′)	122.8(2)	O(2′)−C(3′)−C(4′)	123.1(2)
C(2′)−C(3′)−C(4′)	114.1(3)	C(5′)−C(4′)−O(1′)	124.5(3)
C(5′)−C(4′)−C(3′)	112.5(2)	O(1′)−C(4′)−C(3′)	123.0(3)
C(4′)−C(5′)−S(1′)	111.9(2)	C(4′)−O(1′)−C(6′A)[a]	110.4(3)
C(4′)−O(1′)−C(6′B)[b]	110.3(8)	C(3′)−O(2′)−C(7′)	112.3(2)
C(7′)−C(6′A)[a]−O(1′)	114.9(6)	C(7′)−C(6′B)[b]−O(1′)	117.5(14)
O(2′)−C(7′)−C(6′A)[a]	116.9(4)	C(6′B)[b]−C(7′)−O(2′)	124.0(8)
C(5″)−S(1″)−C(2″)	92.53(13)	C(3″)−C(2″)−C(2)	127.4(2)
C(3″)−C(2″)−S(1″)	109.4(2)	C(2)−C(2″)−S(1″)	123.2(2)
C(2″)−C(3″)−O(2″)	123.3(2)	C(2″)−C(3″)−C(4″)	114.4(2)
O(2″)−C(3″)−C(4″)	122.3(2)	C(5″)−C(4″)−O(1″)	123.9(2)
C(5″)−C(4″)−C(3″)	112.3(2)	O(1″)−C(4″)−C(3″)	123.8(2)
C(4″)−C(5″)−S(1″)	111.4(2)	C(4″)−O(1″)−C(6″)	112.0(2)
C(3″)−O(2″)−C(7″A)[c]	109.9(2)	C(3″)−O(2″)−C(7″B)[d]	111.4(6)
O(1″)−C(6″)−C(7″A)[c]	115.0(3)	O(1″)−C(6″)−C(7″B)[d]	123.7(6)
C(6″)−C(7″A)[c]−O(2″)	114.6(4)	C(6″)−C(7″B)[d]−O(2″)	111.4(10)

[a] Disordered; site occupancy 80%. [b] Disordered; site occupancy 20%. [c] Disordered; site occupancy 75%. [d] Disordered; site occupancy 25%.

Table 5. Bond Lengths (Å) and Angles (deg) for BEDOT-B

C(1)−C(6)	1.399(3)	C(3′)−O(2′)	1.371(3)	C(1)−C(2)	1.399(3)
C(3′)−C(4′)	1.428(3)	C(1)−C(2′)	1.468(2)	C(4′)−C(5′)	1.350(3)
C(2)−C(6)[a]	1.388(3)	C(4′)−O(1′)	1.373(3)	C96)−C(2)[a]	1.388(3)
O(1′)−C(6′)	1.438(3)	S(1′)−C(5′)	1.716(2)	O(2′)−C(7′)	1.447(3)
S(1′)−C(2′)	1.740(2)	C(6′)−C(7′)	1.500(3)	C(2′)−C(3′)	1.362(3)

C(6)C(1)−C(2)	118.2(2)	C(2′)−C(3′)−C(4′)	113.4(2)
C(6)−C(1)−C2′)	121.2(2)	O(2′)−C(3′)−C(4′)	122.4(2)
C(2)−C(1)−C(2′)	120.6(2)	C(5′)−C(4′)−O(1′)	124.1(2)
C(6)[b]−C(2)−C(1)	120.7(2)	C(5′)−C(4′)−C(3′)	113.2(2)
C(2)[b]−C(6)−C(1)	121.1(2)	O(1′)−C(4′)−C(3′)	122.6(2)
C(5′)−S(1′)−C(2′)	92.70(11)	C(4′)−C(5′)−S(1′)	111.0(2)
C(3′)−C(2′)−C(1)	129.8(2)	C(4′)−O(1′)−C(6′)	112.2(2)
C(3′)−C(2′)−S(1′)	109.7(2)	C(3′)−O(2′)−C(7′)	111.3(2)
C(1)−C(2′)−S(1′)	120.5(2)	O(1′)−C(6′)−C(7′)	111.8(2)
C(2′)−C(3′)−O(2′)	124.0(2)	O(2′)−C(7′)−C(6′)	111.0(2)

[a] Atom generated by the symmetry transformation: $1 - x$, $1 - y$, $1 - z$.

Table 6. Electrochemical, Electronic, and Electrochromic Properties of BEDOT Monomers and Polymers

monomer	$E_{onset,m}$	$E_{p,m}$	$E_{1/2,p}$[a]	E_g	color reduced	color oxidized
BEDOT-V	0.36	0.45	0.02	1.4	deep purple	sky blue
TER-EDOT	0.14	0.20	−0.27	1.6	deep blue	sky blue
BEDOT-T	0.30	0.40	−0.50	1.7	deep blue	blue
BEDOT-F	0.32	0.37	−0.09	1.7	deep blue	blue
BEDOT-B	0.61	0.65	0.23	1.8	red	blue-purple
BEDOT-BP	0.66	0.75	0.30	2.3	orange	purple

[a] $E_{1/2,p}$ values are reported for the major redox process of each polymer with a scan rate of 100 mV/s yielding peak-to-peak separations of ≤0.10 V.

BEDOT-V, BEDOT-F, and BEDOT-T have slightly higher, and essentially the same oxidation potentials with $E_{p,m}$'s at ca. 0.4 V. These similarities parallel that of terthiophene and bis(2-thienyl)furan which have a small difference in peak oxidation potentials of 0.07 V.[21] This might be attributed to a balancing of cation-radical stabilization in the thiophene with an enhanced raising of the HOMO in the furan. BEDOT-B and BEDOT-BP have significantly higher peak oxidation potentials than the other monomers studied. While no direct correlation of crystal structure determined torsional angle can be made with oxidation potentials in solution, the observed oxidation potentials scale with the stability of the cation radicals formed and can be related to the ability of the monomers to be planar. It should be noted that the two oxygens of the central EDOT ring in TER-EDOT have a significant effect on the oxidation potential (approximately 0.2 V) when compared to BEDOT-T.

Oxidative Polymerization. The oxidative polymerization, along with the subsequent reversible redox process, of the bis(3,4-ethylenedioxythienyl) monomers is depicted in Scheme 2 using BEDOT-B as an example. The polymerization proceeds through an electrochemically activated step-growth mechanism. The first step involves the formation of a monomer cation radical which is then followed by a coupling polymerization. Electrochemical polymerization and film deposition was carried out using multiple scan cyclic voltammetry. Figure 3 shows the multiple scan cyclic voltammetric polymerization of TER-EDOT. For comparative purposes, the parent heterocycle, 3,4-ethylenedioxythiophene, was electrochemically polymerized under the same conditions and the first and tenth scans are shown as an inset in Figure 3. These results are representative of all of the bis(3,4-ethylenedioxythiophene)arylenes.

Upon multiple cycling of the TER-EDOT solution, a new redox process develops at a lower potential ($E_{1/2,p} = -0.25$ V) due to the reversible redox process of the as-deposited poly(TER-EDOT). The current response of this new redox process continues to increase in intensity upon additional cycling consistent with the deposition of an electroactive polymer onto the surface of the working electrode. Further evidence for the formation of the polymer is the observation of a dark blue (when cycling was stopped at −0.8 V) film on the

(21) Ferraris, J. P.; Hanlon, T. R. *Polymer* **1989**, *30*, 1319.

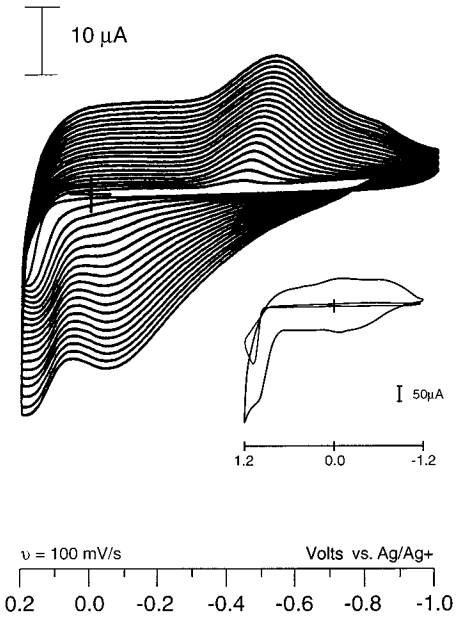

Figure 3. Cyclic voltammetric scanning electropolymerization of 0.01M TER-EDOT in 0.1 M TBAP/CH_3CN cycled at 100 mV/s. Inset shows the first and tenth scans for oxidation and polymerization of 0.01 M EDOT in 0.1 M TBAP/CH_3CN cycled at 100 mV/s.

Scheme 2

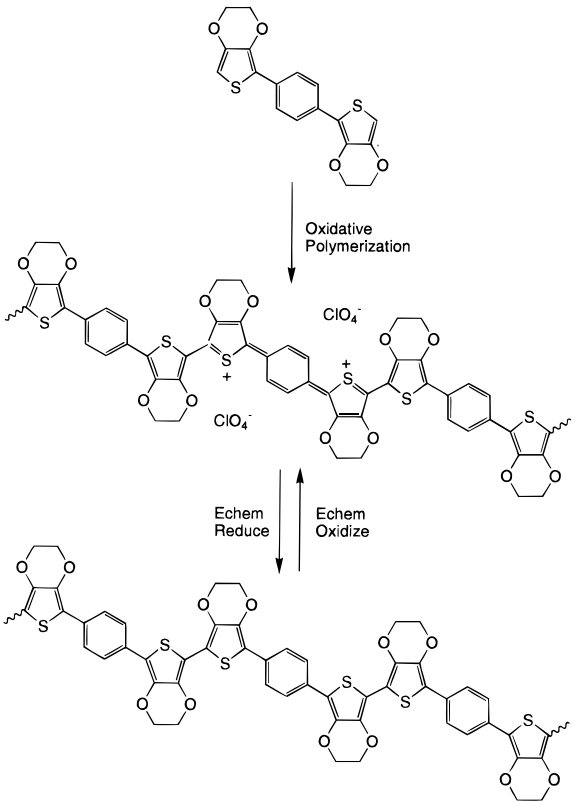

surface of the working electrode. In addition to the $E_{onset,m}$ and $E_{p,m}$ values, Table 6 lists the half-wave redox potentials for the polymers ($E_{1/2,p}$) and the electronic bandgaps (E_g) for all of the systems studied. The low potential polymerization of TER-EDOT is made especially evident by comparison to the parent heterocycle EDOT in the inset to Figure 3. EDOT exhibits an $E_{m,onset}$ of 1.0 V, which is 0.85 V greater than the $E_{m,onset}$ for TER-EDOT. The redox processes for the poly(TER-EDOT) are more distinct than poly(EDOT). This indicates that while the polymers have the same nominal

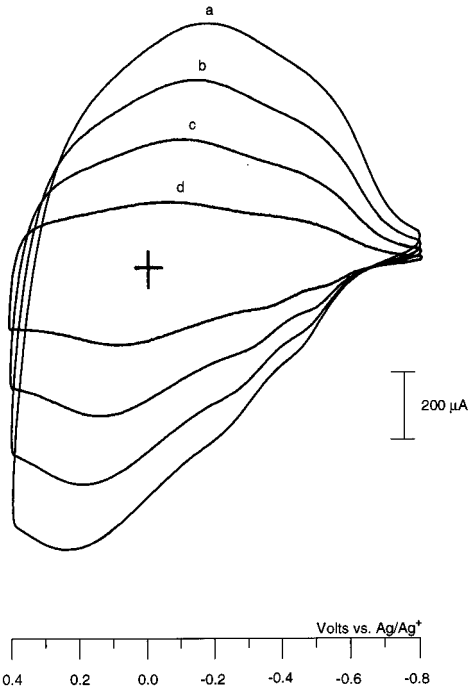

Figure 4. Scan-rate dependence of the cyclic votammetry of poly(BEDOT-V) electrochemically polymerized from a 0.01 M BEDOT-V/0.1 M TBAP/CH_3CN solution using multiple scan (five cycles) cyclic voltammetry. Poly(BEDOT-V) scanned at (a) 400, (b) 300, (c) 200, and (d) 100 mV/s.

repeat unit, electropolymerization and film formation is more efficient using the three-ring monomer.

Perchlorate doped poly(BEDOT-V) and poly(BEDOT-F) were potentiostatically synthesized at the $E_{p,m}$ using TBAP/acetonitrile as the electrolyte, and characterized by elemental analysis, to determine the dopant ion composition per repeat unit incorporated into the polymer. Poly(BEDOT-V) was found to contain 0.69 dopant ion/repeat (0.057 charge/main chain atom) as calculated using the Cl- to -S ratio. Poly(BEDOT-F) was found to contain 0.83 dopant ion/repeat (0.055 charge/main chain atom). These values are similar to those obtained for most polyheterocycles. For example, perchlorate-doped polythiophene typically is found to contain 0.25−0.33 dopant ion/ring (0.050−0.066 charge/main-chain atom).[22]

Polymer Electrochemistry. To isolate and study the polymer redox properties, the electrochemically deposited films were washed with acetonitrile and placed into monomer-free electrolyte solutions. Figure 4 shows a set of cyclic voltammograms for poly(BEDOT-V) at different scan rates and is representative for all the systems studied.

As illustrated by Figure 4, the current is linearly proportional to the scan rate indicating that the polymer, and all electroactive sites, is electrode supported. As can be seen in Table 6, the oxidation potentials of the monomers scale with the half-wave potentials for the redox processes of the polymers. The lowest polymer redox potential was exhibited by poly(TER-EDOT) with an $E_{1/2,p}$ of −0.25 V. This value is close to that obtained for poly(EDOT) (−0.4 V), as expected since these polymers have the same nominal repeat unit. The redox potential is indicative of the ease with which the neutral polymer is converted to the doped form. As such, polymers with especially low redox potentials are

(22) Chung, T.-C.; Kaufman, J. H.; Heeger, A. J.; Wudl, F. *Phys. Rev. B* **1984**, *30*, 702.

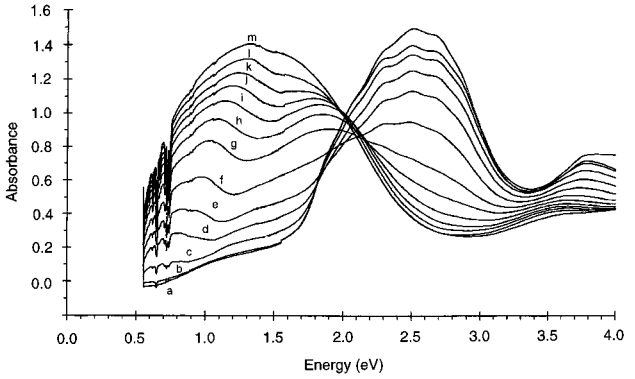

Figure 5. Optoelectrochemical analysis of poly(TER-EDOT) performed in 0.1 M TBAP/CH_3CN. UV−vis−NIR spectra taken at (a) −1.6, (b) −0.9, (c) −0.4, (d) −0.3, (e) −0.2, (f) −0.1, (g) 0.0, (h) 0.1, (i) 0.2, (j) 0.3, (k) 0.4, (l) 0.5, and (m) 1.0 V vs Ag/Ag^+.

found to be highly stable conductors. For example, polypyrrole, which has an $E_{1/2,p}$ quite close to that of poly(EDOT) and poly(TER-EDOT), is well-known for it's conductivity stability. Stability studies carried out on coatings of poly(EDOT) have shown it to have a stability higher than polypyrrole when treated at 100 °C for 25 h.[13a] All of the EDOT-based polymers presented here could be transferred and handled in air while in the oxidized form with no degradation or loss of electrochemistry.

Electronic Structure. Optoelectrochemical studies of the polymers were utilized in order to elucidate the effect of the central unit of the monomers on the π-electron energy levels. Thin films of the polymers were electrochemically deposited onto transparent indium tin oxide (ITO) coated glass plates potentiostatically at the $E_{p,m}$ of the monomer. The spectra were obtained first in the fully reduced state and then sequentially stepped to higher oxidizing potentials. The reversibility of the electronic structure of the polymer was then tested by examining the spectra as the polymers were switched from the oxidized to the reduced form. All of the polymers were shown to behave reversibly. Figure 5 illustrates the optoelectrochemical spectral series obtained for poly(TER-EDOT) while changing from the reduced state to the fully oxidized state. The optical bandgap for each polymer was obtained from the onset of the $\pi-\pi^*$ transition. In the reduced state, poly(TER-EDOT) is opaque purple-blue and has a single broad absorption with an onset at 1.6 eV and λ_{max} at 2.5 eV. Oxidation of the polymer leads to the formation of bipolaronic charge carriers and induces a change in the polymer conformation to a quinoidal structure. The bipolarons are characterized by two new low energy transitions which appear in the vis−NIR region at the expense of the intensity of the $\pi-\pi^*$ transition.

Figure 6 shows the band structure for each polymer, as elucidated from full optoelectrochemical studies, including bipolaron states. Both the valence band to conduction band transition energies (E_{vc}) and valence-to -bipolaron transition energies (E_{b1} and E_{b2}) are listed in Figure 6 as the λ_{max} of the corresponding transition. It should be noted that the E_{vc} represents the most probable transition between bands and is not E_g (previously defined as the onset energy for the transition). The lowest E_{vc} obtained was 2.0 eV for poly(BEDOT-V) which was found to have bipolaron bands with an

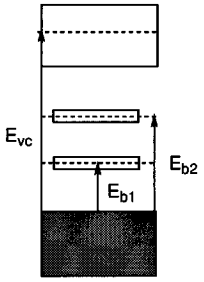

Polymer	$^aE_{vc}$	$^aE_{b1}$	$^aE_{b2}$
Poly(BEDOT-V)	2.0	0.6	1.1
Poly(BEDOT-F)	2.1	0.7	1.4
Poly(BEDOT-T)	2.1	0.7	1.4
Poly(TER-EDOT)	2.5	1.0	1.7
Poly(BEDOT-B)	2.5	0.8	1.8
Poly(BEDOT-BP)	2.8	1.0	2.1

[a] Reported at λ_{max} for each transition

Figure 6. Band structure analysis of the bisEDOT polymers elucidated from optoelectrochemical analysis. All values are given in electronvolts and are reported as the λ_{max} values of the corresponding transition.

especially small difference in energy (ΔE_b = 0.5 eV) relative to the other polymers.[18a] Upon full oxidation, coalescence into a single broad low-energy transition occurs. Upon reduction, the single broad peak returned to two broad transitions at distinct energies. None of the other polymers displayed this behavior, possibly due to a larger separation in energy between the two bipolaron states.

Poly(BEDOT-BP) was found to exhibit the largest E_{vc} of 2.8 eV with the other polymers having intermediate transition energies. Poly(BEDOT-F) and poly(BEDOT-T) exhibited highly similar band structures. Both had E_{vc}'s of 2.1 eV and bipolaron bands emerging at lower energies of 0.7 and 1.4 eV. The energy separation between the bipolaron states was sufficient to prevent coalescence, even at an applied potential of 1.2 V.

Electrochromic Properties. As indicated by the band-structure analysis, these polymers exhibit a spectrum of colors in the neutral form, ranging from deep purple for poly(BEDOT-V) to orange for poly(BEDOT-BP). During redox switching, distinct color changes occur demonstrating the potential utility of these polymers as electrochromic films as noted in Table 6. Further color refinement is possible by considering copolymerization of these monomers.

A thin film (ca. 200 nm thickness) of poly(BEDOT-V) was potentiostatically deposited onto an ITO-coated glass electrode at the $E_{p,m}$, and the polymer was subsequently stepped between the oxidized (E = +0.6 V) and reduced (−0.6 V) forms in 5 s intervals in a 0.1 M TBAP/CH_3CN electrolyte solution. The visible transmittance (600 nm, λ_{max} of the polymer) and charge were monitored as a function of time. The visible transmittance vs time plot is illustrated for the initial double potential steps in Figure 7.

In stepping from the opaque reduced to the transmissive oxidized state, the polymer was found to have a switching time of ca. 2 s in order to effect 100% of the charge and absorbance change. A faster response time of ca. 0.5 s was observed in going from the oxidized to the reduced state. Stepping from the oxidized to the reduced state is inherently faster than stepping from the reduced to the oxidized state. This can be attributed to the ease of charge transport in the conducting film as it is reduced. Reduction of the oxidized polymer may begin at any site within the polymer film. On the other hand, a conducting "front" moves from the polymer: electrode interface to the polymer:electrolyte interface during oxidative doping to the conducting state, an inherently slower process.

Table 7 lists the percent transmittance of the oxidized (T_{ox}) and reduced (T_{red}) forms of the polymer, optical

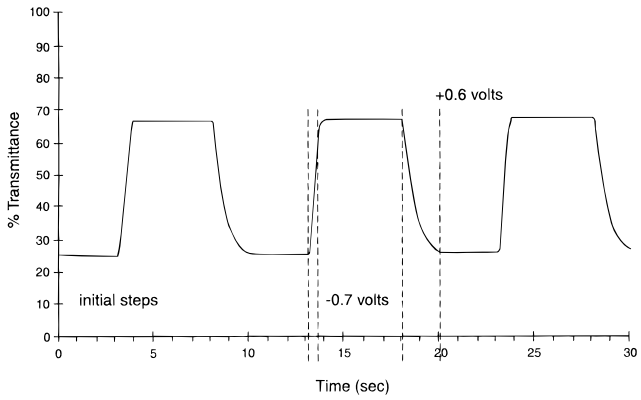

Figure 7. Percent transmittance vs time plot for the double potential stepping of a 200 nm thick film of poly(BEDOT-V) deposited onto an ITO-coated glass plate working electrode. Voltages are reported vs Ag/Ag^+.

Table 7. Double-Potential Stepping Long-Term Stability Data for Poly(BEDOT-V) in 0.1 M TBAP/ACN

S[a]	0	100	200	300	400	600
T_{ox}[b]	25	29	32	36	38	40
T_{red}[b]	68	63	60	60	60	60
ΔT[b]	43	34	28	24	22	20
$\Delta T/\Delta T_0 \cdot 100$	100	79	65	56	51	47
[c]Q_d	19.5	16.0	14.3	12.6	10.2	9.4
[b]$Q_{ds}/Qd_0 \cdot 100$	100	82.0	78.3	64.4	52.2	48.0

[a] S denotes double-potential step number. [b] Values listed as percentages. [c] Charge densities reported in mC/cm^2.

contrast ($\Delta T = T_{red} - T_{ox}$), percent optical transmittance efficiency ($\Delta T_S/\Delta T_0 \cdot 100$, where ΔT_S = percent optical transmittance difference at a specific double-potential step, S, and ΔT_0 = percent optical transmittance difference at the initial double-potential step), total charge density passed during a double-potential step (Q_d), and the percent Coulombic efficiency ($Q_{dS}/Q_{d0} \cdot 100$, where Q_{dS} = charge density at double potential step, S, and Q_{d0} = charge density for the initial double potential step) for a 0.75 cm^2 film . The polymer was found to retain an optical transmittance efficiency of 47% and a Coulombic efficiency of 48.0%, after 600 double-potential steps. While this experiment demonstrates the polymer's electrochromism to be stable to a number of transitions between the oxidized and reduced states, these results are not optimized. Further studies in electrochromic devices with controlled counter electrode reactions, and hermetically sealed, are in progress.

In conclusion, a series of extended multiring conjugation monomers containing terminal EDOTs have been synthesized and electropolymerized to yield electroactive and electrochromic polymers. These monomers have oxidation potentials ranging from 0.2 V (TER-EDOT) to 0.75 V (BEDOT-BP) vs Ag/Ag^+, making them 0.9 and 0.35 V lower than that of EDOT itself. Multiple-scan cyclic voltammetric polymerization of the BEDOT monomers yielded electroactive polymers with low redox potentials. Scan-rate dependency of the polymers indicated that the films were electroactive and electrode supported. Optoelectrochemical analysis provided band structures and indicated that the electronic states of the polymers attained at different electrochemical potentials was reversible. Although the only polymer found to have a bandgap lower than that of poly(EDOT) was poly(BEDOT-V), the other polymers exhibited a diverse range of colors which could prove useful in electrochromic devices. To test the potential utility of these polymers in electrochromic devices, the lowest bandgap polymer was chosen for an optical contrast and cycling rate experiment. While typical response times measured for polymers in electrochromic displays or mirrors are of the order of a few seconds,[23] a 200 nm thick poly(BEDOT-V) film was found to cycle rapidly (under 2 s to effect 100% of the charge and absorbance change) between its conductive and insulating states with an initial optical contrast of 40%.

Experimental Section

Reagents. EDOT was used as purchased from Bayer. 1,4-Dibromobenzene and 4,4′-dibromobiphenyl were recrystallized from chloroform ($CHCl_3$) before use. *N*-Bromosuccinimide was recrystallized from distilled water and vacuum dried at 70 °C for 24 h. Tetrabutylammonium perchlorate (TBAP) used for optoelectrochemical analysis was melt dried under vacuum, and TBAP used for all other electrochemical characterization was recrystallized from ethanol and vacuum dried. The melt drying of organic perchlorates is extremely dangerous and should be carried out behind a protective shield. Reagent-grade acetonitrile (ACN) purchased from Fisher was distilled over calcium hydride (CaH_2) under nitrogen. Tetrahydrofuran (THF) purchased from Fisher was distilled over sodium/benzophenone ketyl under argon. Furan, 2,5-dibromothiophene, *n*-butyllithium (2.5 M in hexanes), magnesium bromide etherate ($MgBr_2 \cdot Et_2O$), bis(diphenylphosphino)propanenickel(II) chloride, bromine, *trans*-dichloroethylene, and anhydrous dimethylformamide (DMF) were used as received from Aldrich. Prior to all experimentation, apparati were dried in an oven and purged with either nitrogen or argon. All reactions were performed in an inert atmosphere of either nitrogen or argon.

2,5-Dibromofuran. To a pressure-equalizing addition funnel was added 47 g (0.297 mol) of bromine dissolved in 60 mL of anhydrous DMF. The bromine/DMF solution was added dropwise to a solution of furan (10.0 g, 0.147 mol) dissolved in 50 mL of DMF over 45 min, after which the reaction mixture was heated to 60 °C. After 30 min the crude reaction mixture was added to approximately 1 L of ice water. This was then washed three times with 100 mL of pentane. The pentane layers were combined and evaporated to dryness. To the crude product was added 2 mL of dimethylaniline. The product, 2,5-dibromofuran, was distilled under reduced pressure (55 °C, 10 mmHg) to give 7.0 g (21%) purified yield. The product was characterized by ^1H and ^{13}C NMR.

2,5-Dibromo-3,4-ethylenedioxythiophene. A 50:50 solution of 50 mL of $CHCl_3$ and 50 mL of glacial acetic acid was prepared. To this solution was added 3.0 g (0.021 mol) of EDOT followed by 8.0 g (0.045 mol) of NBS. After about 2 minutes the solution had changed from clear and colorless to clear and yellow. After approximately 2.5 h 200 mL of distilled water was added to the reaction mixture. The organic layer was a green-blue color. The organic layer was separated and washed again with 100 mL of distilled water. The solution was then neutralized with sodium bicarbonate until bubbling ceased. The residual sodium bicarbonate was filtered and then the organic layer was separated and the $CHCl_3$ was distilled off. The dark blue solid obtained was purified by placing it in boiling ethanol. This was then filtered to give 4.1 g (64.8%) of purified product. ^1H NMR (DMSO-d_6) 4.07 (s).

(*E*)-1,2-Bis(2-(3,4-ethylenedioxy)thienyl)vinylene, BEDOT-V. A solution of EDOT (9.23 g, 0.065 mol) in THF (200 mL) under nitrogen was cooled to −78 °C via a dry ice/acetone cooling bath. To the stirred precooled solution was added 34 mL (0.068 mol) of *n*-butyllithium via syringe. After 45 min, the reaction mixture was allowed to warm to 0 °C via ice bath, after which 16.8 g (0.065 mol) of $MgBr_2 \cdot Et_2O$ was added in one portion. After 45 min, 3.14 g (0.032 mol) of *trans*-dichloroethylene and 0.50 g (0.92 mmol, 1.4 mol %) of catalyst, $NiCl_2 \cdot$dppp, was added. The reaction was allowed to warm slowly to room temperature. Immediately after the addition of catalyst the solution had changed in color from dull yellow

(23) Monk, P. M. S.; Mortimer, R. J.; Rosseinsky, D. R. *Electrochromism: Fundamentals and Applications;* VCH: Weinheim, 1995.

to orange. After approximately 0.5 h the reaction mixture turned red clear and eventually after 2 h the reaction mixture had turned a desirable black-brown. The reaction was allowed to continue for 48 h, after which, it was poured into 200 mL of water and 100 mL of pentane. The product precipitated out between the aqueous and organic layer and was filtered, washed with pentane, and further purified by column chromatography using $CHCl_3$ as the eluent to give 5.8 g (58%) purified yellow-orange product; mp 133−135 °C. λ_{max} = 359 nm; ^{1}H NMR (DMSO-d_6) 4.2(m, 2H), 4.25(m, 2H), 6.5(s, 1H), 6.75(s, 1H); ^{13}C NMR ($CDCl_3$) 64.9, 65.0, 97.23, 116.17, 117.56, 139.09, 142.20. Elemental anal. calcd for $C_{14}H_{10}S_2O_4$: C, 54.50; H, 3.93; S, 20.82. Found: C, 54.10; H, 3.81; S, 20.50. FAB-HRMS calcd for $C_{14}H_{12}S_2O_4$: 308.0177. found: 308.0189.

1,4-Bis(2-(3,4-ethylenedioxy)thienyl)benzene, BEDOT-B. BEDOT-B was prepared in a similar manner as BEDOT-V except that the reaction time was reduced to 18 h. The amounts of reagents used were 1.00 g (7.04 mmol) of EDOT, 40 mL of THF, 2.8 mL (7.00 mmol) of 2.5 M *n*-BuLi, 1.85 g (7.00 mmol) of $MgBr_2{\cdot}Et_2O$, 0.060 g (0.11 mmol, 1.5 mol %) $NiCl_2$·dppp, and 0.83 g (3.50 mmol) of dibromobenzene. Workup was similar to BEDOT-V. The product obtained after chromatography was a brown solid, 0.92 g (73.6%), mp 179−180 °C; λ_{max} = 344 nm; ^{1}H NMR (DMSO-d_6) 4.25 (m, 2H), 4.31 (m, 2H), 6.62 (s, 1H), 7.65 (s, 2H); ^{13}C NMR (DMSO-d_6) 64.64, 65.23, 98.48, 116.05, 126.02, 131.49, 139.03, 142.70. FAB-HRMS calcd for $C_{18}H_{14}O_4S_2$: 358.0333. Found: 358.0336.

4,4′-Bis(2-(3,4-ethylenedioxy)thienyl)biphenyl, BEDOT-BP. BEDOT-BP was prepared in a manner similar to that for BEDOT-B. After column chromatography, 1.25 g (82%) of the yellow product was collected (mp 186−189 °C) λ_{max} = 342 nm; ^{1}H NMR ($CDCl_3$) 4.25 (m, 2H), 4.36 (m, 2H), 6.32 (s, 1H), 7.65 (d, 2H), 7.81 (d, 2H); ^{13}C NMR ($CDCl_3$) 64.64, 65.28, 98.47, 117.15, 126.23, 127.04, 132.54, 138.12, 138.59, 141.97. FAB-HRMS calcd for $C_{24}H_{18}O_4S_2$: 434.0647. Found 434.0651.

2,5-Bis(2-(3,4-ethylenedioxy)thienyl)furan, BEDOT-F. BEDOT-F was prepared in a manner similar to that for BEDOT-B. The amounts of reagents used were 4.00 g (0.0282 mol) of EDOT, 180 mL of THF, 11.3 mL of 2.5 M *n*-BuLi, 7.3 g (0.0282 mol) of $MgBr_2{\cdot}Et_2O$, 0.3 g (0.56 mmol, 1.9 mol %) $NiCl_2$·dppp, and 3.19 g (0.0141 mol) of 2,5-dibromofuran. After precipitation from water/pentane, a light brown solid (3.4 g, 69.2%) was obtained (mp 175−176 °C); λ_{max} = 362; ^{1}H NMR ($CDCl_3$) 4.25 (s, 2H), 4.35 (s, 2H), 6.28 (s, 1H), 6.67 (s, 1H); ^{13}C NMR ($CDCl_3$) 64.60, 64.92, 97.46, 104.88, 108.20, 137.20, 141.78, 145.60. Elemental anal. calcd for $C_{16}H_{12}O_5S_2$: C, 55.12; H, 3.48; S, 18.43. Found: C, 55.13; H, 3.51; S, 18.37. FAB-HRMS calcd for $C_{16}H_{12}O_5S_2$: 348.0126, found 348.0147.

2,5-Bis(2-(3,4-ethylenedioxy)thienyl)thiophene, BEDOT-T. BEDOT-T was prepared in a manner similar to that for BEDOT-B except the reaction time was increased to 48 h. The amounts of reagents used were 30 g (0.211 mol) of EDOT, 400 mL of THF, 85 mL (0.220 mol) of 2.5 M *n*-BuLi, 57 g (0.220 mol) of $MgBr_2{\cdot}Et_2O$, 1.0 g (1.87 mmol, 8.5 mol%) of $NiCl_2$·dppp, and 27 g (0.120 mol) of 2,5-dibromothiophene. After precipitation from water/pentane and pentane washing a canary yellow product (24.5 g, 63.7%) was obtained (mp 103−105 °C); λ_{max} = 374 nm; ^{1}H NMR ($CDCl_3$) 4.25 (s, 2H), 4.35(s, 2H), 6.25 (s, 1H), 7.14 (s, 1H); ^{13}C NMR ($CDCl_3$) 65.2, 65.5, 97.2, 112.3, 123.8, 134.1, 137.9, 142.3. Elemental anal. calcd for $C_{16}H_{12}O_4S_3$: C, 52.74; H, 3.29; S, 26.3. Found: C, 52.40; H, 3.29; S, 25.69. FAB-HRMS calcd for $C_{16}H_{12}O_4S_3$: 363.9898. Found: 363.9896.

2,2′:5′,2″-Ter(3,4-ethylenedioxy)thiophene, TER-EDOT. The procedure to prepare TER-EDOT was similar to that for BEDOT-B. The amounts of reagents used were 1.33 g (9.37 mmol) of EDOT, 50 mL of THF, 3.7 mL (9.25 mmol) of 2.5 M *n*-BuLi, 2.5 g (9.68 mmol) of $MgBr_2{\cdot}Et_2O$, 0.10 g (0.187 mmol, 1.9 mol %) of $NiCl_2$·dppp, and 1.4 g (4.67 mmol) of 2,5-dibromoEDOT. After precipitation from water/pentane and pentane washing a medium brown product (2.6 g, 65.5%). λ_{max} = 400 nm; ^{1}H NMR (DMSO-d_6) 4.23 (m, 6H), 6.54 (s, 1H); FAB-HRMS calcd for $C_{18}H_{14}O_6S_3$: 421.9953. Found: 421.9963.

Instrumentation. All NMR spectra were performed using either a Varian VXR-300 or a General Electric QE-300 using either deuterated chloroform ($CDCl_3$) or deuterated dimethylsulfoxide (DMSO-d_6) as a solvent unless otherwise stated. All experiments involving the use of a potentiostat were performed on a EG&G Princeton Applied Research Model 273 potentiostat/galvanostat. UV−vis−NIR data along with optoelectronical spectra were obtained using a Varian Cary 5 UV−vis−NIR spectrophotometer.

X-ray Crystallography: Data Collection, Structure Solution, and Refinement. All measurements were made with a Nicolet P4s diffractometer using graphite monochromatized Mo Kα (λ = 0.710 73 Å) radiation. Cell parameters were obtained by least-squares refinement of the setting angles of at least 25 accurately centered reflections with $2\theta > 25°$. Throughout data collections (ω scans) the intensities of three standard reflections were monitored at regular intervals, and this indicated no significant crystal decomposition. Intensities were corrected for Lorentz and polarization effects but not for absorption. The structures were solved by direct methods using SHELXS-90[24] and refined on F^2 using all data by full-matrix least-squares procedures with SHELXL-93.[25] All non-hydrogen atoms were refined with anisotropic displacement parameters. The occupancies of disordered atoms were obtained by refinement. Hydrogen atoms were included in calculated positions with isotropic displacement parameters 1.2 times the isotropic equivalent of their carrier carbons. The functions minimized were $\Sigma w(F_o^2 - F_c^2)$, with $w = [\sigma^2(F_o^2) + aP^2]^{-1}$ where $P = [\max(F_o^2) + 2F_c^2]/3$. Final non-hydrogen atom coordinates are given in Tables 2 and 3 for BEDOT-V and BEDOT-B, respectively. Full tables of atom coordinates, thermal parameters, bond lengths, and bond angles and structure factors are available from the author P.J.S. and have been deposited with the Cambridge Crystallographic Data Base.

Electrochemistry. A 0.006 cm^2 platinum button working electrode, a 1 cm^2 platinum plate counter electrode, and a Ag/Ag^+ (0.010 M AgNO3/0.10 M TBAP) nonaqueous reference electrode were used for cyclic voltammetry experiments. All electrochemical potentials will be reported relative to the Ag/Ag^+ reference electrode. Prior to all electrochemistry, solutions were purged with argon and during electrochemistry an argon blanket was maintained over the solution. The optical spectrum of each polymer, as a function of injected charge, was obtained using indium tin oxide (ITO) coated conducting glass as a working electrode. Films were electrochemically polymerized onto the ITO-coated glass via constant potential until a desired charge density was obtained. Then, the ITO with deposited polymer was placed into a quartz cuvette with monomer-free electrolyte, and the counter electrode was a platinum plate with a 1 cm diameter hole in the center. A silver wire was used as a quasi-reference electrode. All optoelectronic experiments were performed in a nitrogen atmosphere.

Acknowledgment. This work was supported by grants from the National Science foundation (CHE 9307732) and AFOSR (F49620-920-J-0509).

Supporting Information Available: Listings of anisotropic displacement parameters, hydrogen coordinates and isotropic displacement parameters are provided for BEDOT-V and BEDOT-B (4 pages). Ordering information is given on any current masthead page.

CM9504798

(24) Sheldrick, G. M. *Acta Crystallogr., Sect. A* **1990**, *46*, 467.
(25) Sheldrick, G. M., SHELXL-93, University of Gottingen, 1993.